



A novel technique of cervical pedicle screw placement with a pilot screw under the guidance of intraoperative 3D imaging from C-arm cone-beam CT without navigation for safe and accurate insertion

Masahiko Takahata¹ · Katsuhisa Yamada¹ · Iwata Akira¹ · Tsutomu Endo¹ · Hideki Sudo¹ · Hidetoki Yokoyama² · Norimasa Iwasaki¹

Received: 1 February 2018 / Accepted: 16 July 2018 / Published online: 23 July 2018
© Springer-Verlag GmbH Germany, part of Springer Nature 2018

Abstract

Purpose The cervical pedicle screw (CPS) requires careful and accurate placement because of the critical risk for neurovascular injury. This study aimed to introduce and evaluate the safety and efficacy of a new CPS placement technique using intraoperative C-arm cone-beam CT (CBCT) and a pilot screw without navigation system.

Methods This was a case–control study to compare the accuracy and safety of intraoperative C-arm CBCT-guided CPS placement with freehand CPS placement under lateral fluoroscopy using control data from a previous multicenter study. A total of 166 CPSs were inserted under intraoperative C-arm CBCT guidance in 48 consecutive patients (20 rheumatoid arthritis, 16 degenerative spinal disorders, 6 spinal tumor, 2 congenital deformity, 2 ossification of posterior longitudinal ligament, and 2 fracture dislocation). Accuracy and safety of CPS placement were assessed.

Results The overall malposition rate was 2.4% (4 screws in grade 1: malposition by less than half-screw diameter, 0 in grade 2: malposition by more than half-screw diameter), which was significantly lower than the reported malposition rate of 14.8% in lateral fluoroscopy-guided freehand placement. There were no complications directly related to CPS insertion. The average estimated effective radiation dose per surgery was 14.7 mSv.

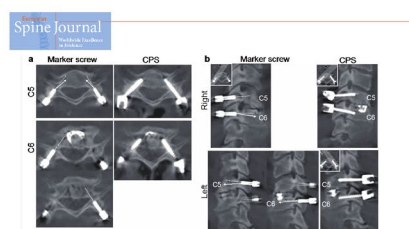
Conclusions The novel technique enables intraoperative adjustment of the trajectory of the CPS as well as confirmation of the CPS path before penetrating the isthmus of the pedicle, resulting in accurate and safe CPS placement, which outweighs the demerits of radiation exposure.

Graphical abstract These slides can be retrieved under Electronic Supplementary Material.

Key points

1. This study introduced a new intraoperative cone-beam CT guided cervical pedicle screw placement technique.
2. The cone-beam CT guided CPS placement was safer and more reliable compared to fluoroscopy guided free hand CPS placement.
3. Since the information obtained from intraoperative cone-beam CT is a real-time accurate representation, it offers highly reliable 3D guidance for CPS placement, which outweighs the demerits of radiation exposure.

Masahiko Takahata, Katsuhisa Yamada, Iwata Akira, Tsutomu Endo, Hideki Sudo, Hidetoki Yokoyama, Norimasa Iwasaki (2018) A novel technique of cervical pedicle screw placement with a pilot screw under the guidance of intraoperative 3D imaging from C-arm cone-beam CT without navigation for safe and accurate insertion. *Eur Spine J*; Springer



Masahiko Takahata, Katsuhisa Yamada, Iwata Akira, Tsutomu Endo, Hideki Sudo, Hidetoki Yokoyama, Norimasa Iwasaki (2018) A novel technique of cervical pedicle screw placement with a pilot screw under the guidance of intraoperative 3D imaging from C-arm cone-beam CT without navigation for safe and accurate insertion. *Eur Spine J*; Springer

Take Home Messages

1. The information obtained from intraoperative cone-beam CT is a real-time accurate representation. Therefore, it offers highly reliable 3D guidance for CPS placement, which outweighs the demerits of radiation exposure.
2. Cone-beam CT guided CPS placement can ensure its safety as well as provide a more reliable anchor for cervical spinal reconstruction compared to conventional fluoroscopy guided free hand CPS insertion.

Masahiko Takahata, Katsuhisa Yamada, Iwata Akira, Tsutomu Endo, Hideki Sudo, Hidetoki Yokoyama, Norimasa Iwasaki (2018) A novel technique of cervical pedicle screw placement with a pilot screw under the guidance of intraoperative 3D imaging from C-arm cone-beam CT without navigation for safe and accurate insertion. *Eur Spine J*; Springer

Keywords Cervical pedicle screw · C-arm cone-beam CT · CT guidance · Navigation · 3D fluoroscopy

Electronic supplementary material The online version of this article (<https://doi.org/10.1007/s00586-018-5706-x>) contains supplementary material, which is available to authorized users.

Extended author information available on the last page of the article

Introduction

Despite considerable risk of neurovascular injury, particularly vertebral artery injury, in cervical pedicle screw (CPS) placement [1–4], CPS is an attractive spinal fixation device due to its biomechanical superiority over other spinal anchors [5–8]. Since the efficacy of CPS in cervical spine reconstruction surgery was first demonstrated in the 1990s [7, 9], numerous techniques have been developed to improve the accuracy of CPS placement. Freehand placement of CPS under fluoroscopy may be the most widely used technique [1, 4, 10–12]; however, our multicenter study demonstrated a malposition ratio of 14.8% [2]. Malposition of CPS can occur even in cases performed by experienced surgeons. Most cases requiring cervical spinal reconstructive surgery using CPS lack normal bony landmark and bone marrow cavity due to degenerative changes, destructive bone lesions or congenital deformity. Navigation systems are getting popular and have successfully improved the accuracy of CPS placement compared to the freehand technique; however, the ratio of CPS misplacement still ranges from 1 to 3% [13–15]. This may be attributable to the segmental movement or instability during insertion of CPS, which impairs accuracy of navigation guidance. Therefore, other tools or techniques, which can secure an accurate and safe placement of CPS, are needed.

In recent years, the equipment for intraoperative three-dimensional (3D) imaging from C-arm cone-beam computed tomography (CBCT) has been established all over the world, applicable to various fields such as vascular, brain, and orthopedic surgery [13, 16–19]. This system enables the surgeons to visualize the cervical spine using multiplanar reconstruction images during surgery and can be applicable to CT-guided insertion of CPS as well as postprocedural confirmation of the CPS position before completing the surgery.

In the current study, we aimed to examine the accuracy and safety of a new CPS placement technique using intraoperative 3D imaging from C-arm CBCT and a pilot screw without navigation system. Secondarily we compared the accuracy of the technique to that of freehand placement of CPS under lateral fluoroscopy in historical controls from a previous multicenter study.

Materials and methods

Study design and patients

This was a case–control study to compare the accuracy and safety of intraoperative C-arm CBCT-guided CPS

placement with freehand placement of CPSs under lateral fluoroscopy using historical control data of a previous multicenter study [2]. This study was approved by the appropriate institutional review board.

From January 2013 to July 2017, 48 consecutive patients with cervical disorders who underwent cervical reconstruction surgery using CPSs at our institution were enrolled. There were 32 women and 16 men, with average age at surgery of 60.7 (range: 21–82) years. There were 20 patients with rheumatoid arthritis (RA), 16 with degenerative spondylosis including spondylolisthesis, kyphosis, and athetotic cerebral palsy, 6 with spinal tumors, 2 with congenital deformity, 2 with ossification of posterior longitudinal ligament (OPLL), and 2 with fracture dislocation. Historical control group comprised 283 patients with 1065 CPSs.

Procedure

Equipment

All surgeries were performed using the hybrid operating room (OR), which is equipped with a 3D flat-panel C-arm system (INFX-8000H, Toshiba, Tokyo, Japan) and integrated operating table (Maquet Magnus 1180, NJ, USA). The system can be used as a standard C-arm for acquiring two-dimensional (2D) high-resolution fluoroscopic images and can obtain 3D volumetric CT-like images by automatic rotation around the table.

Preoperative planning

Since an appropriate entry point of CPS is the key to create screw path, we preoperatively planned the entry point and trajectory of CPS using a 3D-visual guidance system for pedicle screw (3D-VG TIPS, Z-view Vega, Lexi, co. Ltd, Tokyo, Japan) in each pedicle as previously reported [21]. Briefly, 3D-VG TIPS used preoperative CT data of the cervical spine and anatomical axis of each pedicle analyzed by volume-rendered 3D models, as with existing navigation systems, and both the ideal entry point and trajectory of each PS were visualized on the surface of 3D-rendered images. This preoperative planning was useful to determine whether pedicle was available for CPS placement and to determine the length and diameter of CPS. Small pedicles with external diameter less than 3.5 mm did not allow CPS insertion.

Surgical technique

Concept and procedure of C-arm CBCT-guided CPS insertion are shown in Figs. 1 and 2.

1. Determination of entry point.

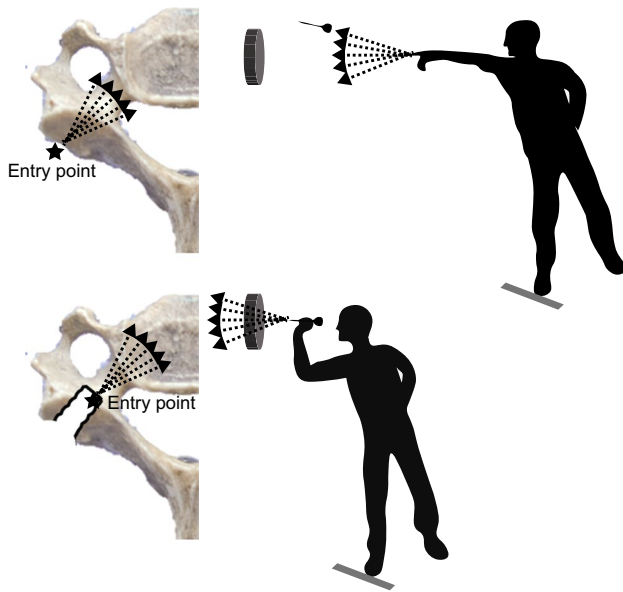


Fig. 1 Concept of the C-arm CBCT-guided CPS placement technique

After exposing the posterior aspect of cervical spine, entry points of CPS were determined according to the 3D-VG TIPS. Cephalocaudal positions of entry points were confirmed by lateral fluoroscopic imaging. Entry point was drilled using the high-speed diamond burr with a 3-mm head.

2. Creating pilot hole and intraoperative C-arm CBCT

Custom-made 10-mm-long cannulated titanium (Ti) marker screws with a diameter of 3 mm (Fig. 3) were inserted toward the pedicle under lateral fluoroscopy. The marker screw was long enough to reach close to the entrance of pedicle but not to breach the transverse foramen to avoid vertebral artery injury. The use of 10-mm length for the marker screw was validated by measuring the critical range of CPS path, which was defined as the region corresponding to the transverse foramen of C3, C4, C5, and C6 vertebrae in all patients. Critical range was defined as depth from the entry point (Supplemental Table 1).

The marker screw was also designed to work as a radiopaque pedicle marker for CT guidance. Intraoperative 3D volumetric CT-like images were obtained, and the trajectory of the pilot hole visualized by the marker screw was three-dimensionally assessed by multiplanar images of CBCT.

3. Pedicle probing

The creation of pilot hole by the marker screw is based on the funnel technique [22], which makes it easier to find the cancellous channel of the pedicle. If the marker screw headed down the right path, we could insert the ball tip guidewire through the cannulated marker screw. If the marker screw headed in the wrong direction, it was removed, and the surgeon then inserted the curved pedicle probe into the pilot hole. The direction of the pedicle probe was adjusted with its tip heading toward the correct direction based on the intraoperative CT-like images.

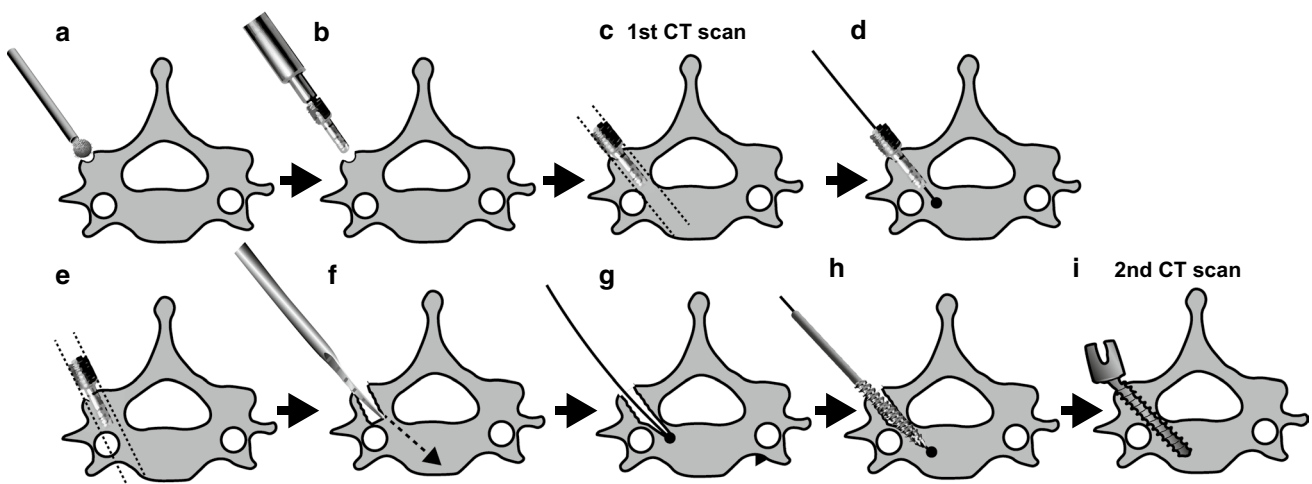


Fig. 2 Procedure of C-arm CBCT-guided CPS placement using custom-made marker screw. **a** Entry point was made using a high-speed drill. **b** Insertion of the Ti marker screw using freehand technique with lateral fluoroscopy. **c** First intraoperative cone-beam CT to assess direction of pilot hole, which was visualized by the marker screw. **d** If the marker screw headed down the right path, the ball tip guidewire was inserted through the cannulated marker screw, and

steps (e–g) were skipped, directly proceeding to step (h). **e** If the marker screw headed in the wrong direction, the marker screw was removed and **f** the curved pedicle probe was inserted by adjusting its trajectory with reference to the intraoperative CT-like images. **g** Insertion of the ball tip guidewire. **h** Tapping of the screw path using cannulated tap driver along the guidewire. **f** Insertion of CPS

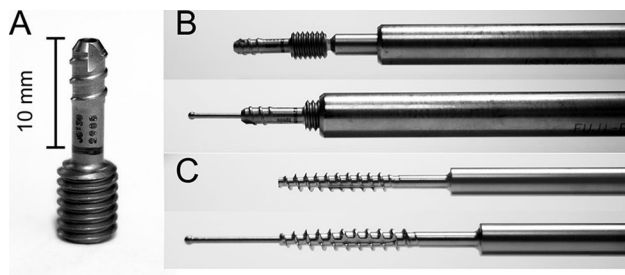


Fig. 3 Custom-made titanium marker screw. **a** Appearance. **b** The marker screw was attached to the cannulated driver, in which the ball tip guide wire could pass through. **c** Cannulated tap driver with a diameter of 3.5 mm and ball tip guide wire

and penetrated the pedicle. When the images indicated the need to adjust the trajectory more medially and caudally in the right-side pedicle, the surgeon adjusted the tip of the curved pedicle probe to a 7–8 o'clock direction and penetrated the pedicle using a pedicle probe.

4. Tapping the screw path and CPS placement

The ball-tipped guidewire was inserted into the hole, and the screw path was tapped by a cannulated tap driver. The ball-tipped guidewire was also used to ensure that pedicle wall was not violated. CPS was then inserted.

5. Confirmation of CPS position

The positions of CPS were confirmed by a second CBCT before completing the surgery.

Evaluation

Placement accuracy of CPS was evaluated by multiplanar CT-like images obtained in the 2nd CBCT during surgery and was classified into three grades: grade 0 (G-0): correct placement, grade 1 (G-1): malposition by less than half-screw diameter, and grade 2 (G-2): malposition by more than half-screw diameter [2]. Screw malposition at each spinal level was also classified into four categories according to the direction of malposition; medial, lateral, superior, and inferior. Malposition rates of CPSs were evaluated from C2 to C7 in different pathological conditions including rheumatoid arthritis, spondylosis, and miscellaneous. Malposition rates of CPSs by intraoperative cone-beam CT-guided placement were compared to those by freehand placement under lateral fluoroscopy using historical control data. P values less than 0.05 were regarded as statistically significant.

Intraoperative and postoperative complications either related or unrelated to CPS placement were also evaluated retrospectively.

The total radiation dose during surgery and the preoperative CT angiography was also evaluated. The effective dose was calculated with tissue weighting factors from

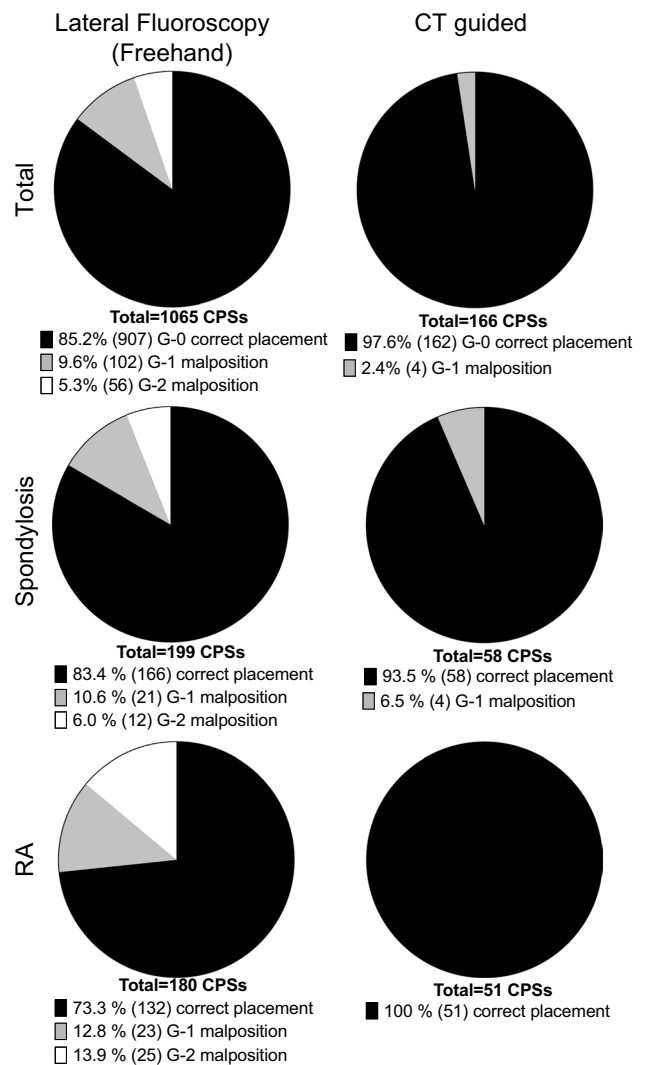


Fig. 4 Comparison of the malposition ratio between C-arm CBCT-guided placement technique and freehand technique under lateral fluoroscopic guidance (historical control data). Malposition ratios in patients with spondylosis, or rheumatoid arthritis and total malposition ratio are shown

publication 103 of the International Commission on Radiological Protection [20, 21].

Results

A total of 166 CPSs were inserted under intraoperative C-arm CBCT guidance in 48 patients with cervical disorders. Overall malposition rate of CPSs by intraoperative C-arm CBCT-guided placement was 2.4% (4/166 CPSs), significantly lower than the malposition rate by freehand technique under lateral fluoroscopic guidance (14.8%—historical control data) (Fig. 4). Of note is that 43.4% (72/166) of the CPSs required trajectory adjustment after 1st intraoperative

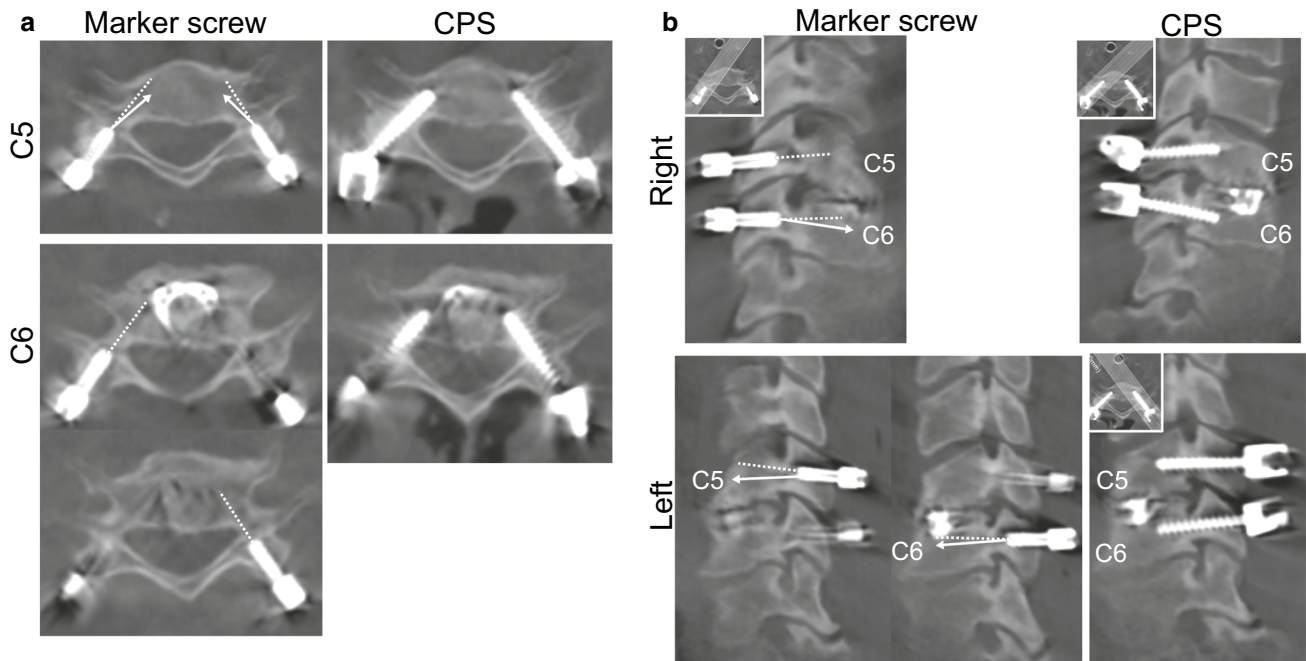


Fig. 5 A 47-year-old man with pseudoarthrosis at C4-5 after anterior discectomy and fusion underwent posterior foraminotomy and fusion with CPSs at C4-5. Axial images at C5 and C6 (**a**) and sagittal images along the pedicle axis (**b**) of intraoperative C-arm CBCT scans are shown. On the CT-like images with the marker screws,

which were obtained before inserting the pedicle probe, white dotted lines indicate the trajectory of marker screws and white arrows indicate the course, which the surgeon corrected to insert the pedicle probe. CT-like images show that CPSs were placed appropriately in the cervical pedicles

CBCT scan, which resulted in excellent accuracy of final CPS placement (Fig. 5).

Malposition of CPSs was identified in 4 screws in 4 patients (1 screw in each patient) with degenerative spondylolisthesis (Fig. 6). All 4 screws were judged noncritical G-1 (less than half-screw diameter) perforations by 2nd intraoperative CBCT and were left unchanged. The level of malpositioned CPSs was 3 for C4 and 1 for C6. No complications associated with G-1 screw malposition developed after surgery. There were no G-2 malpositioned CPSs.

With respect to pathological conditions, malposition of CPS occurred only in patients with degenerative spondylotic conditions (Table 1). Malposition ratio of CPSs in patients with spondylosis was 6.5% by intraoperative C-arm CBCT-guided placement, which was significantly lower than the malposition ratio of 16.6% by freehand technique. The highest malposition ratio of 26.7% was reported in patients with RA by freehand placement under fluoroscopy, while all 51 CPSs in 20 patients with RA were placed in the appropriate position by intraoperative C-arm CBCT-guided placement.

As to the direction of screw malposition, all 4 malpositioned CPSs were laterally placed. There was no screw placed inferiorly, superiorly, or medially.

Surgery-related complications were C5 nerve palsy in 2 patients and lingual edema with airway obstruction in 1 patient. The cause of lingual edema could not be identified

but was estimated to be laceration by the bite block. There was no vertebral artery injury, hematoma, and postoperative infection in patients of this study.

C-arm CBCT was obtained twice in all 47 patients and three times in 1 patient to evaluate the position and direction of the marker screw before inserting CPS and to ensure that the position and direction of CPS after instrumentation were complete. The average radiation dose and estimated effective dose during surgery, including lateral fluoroscopy and 2 times C-arm CBCT scans, were 103 ± 71.3 mGy/surgery and 9.7 ± 6.5 mSv, respectively. To evaluate the vertebral artery as well as bone geometry, all patients underwent a preoperative cervical CT angiography, resulting in a mean volumetric CT dose index ($CTDI_{vol}$) of 82.4 ± 84.3 mGy and a mean dose-length product of 643.1 ± 738.1 mGy cm, which corresponds to an estimated effective dose of 3.8 ± 4.4 mSv. Collectively, for completion of the surgery, the total radiation dose and estimated effective dose (per surgery) were 177.0 ± 106.2 mGy and 14.7 ± 7.9 mSv, respectively.

Discussion

In the present study, we introduced a new intraoperative C-arm CBCT-guided CPS placement technique for safer and more reliable CPS placement. Since the information

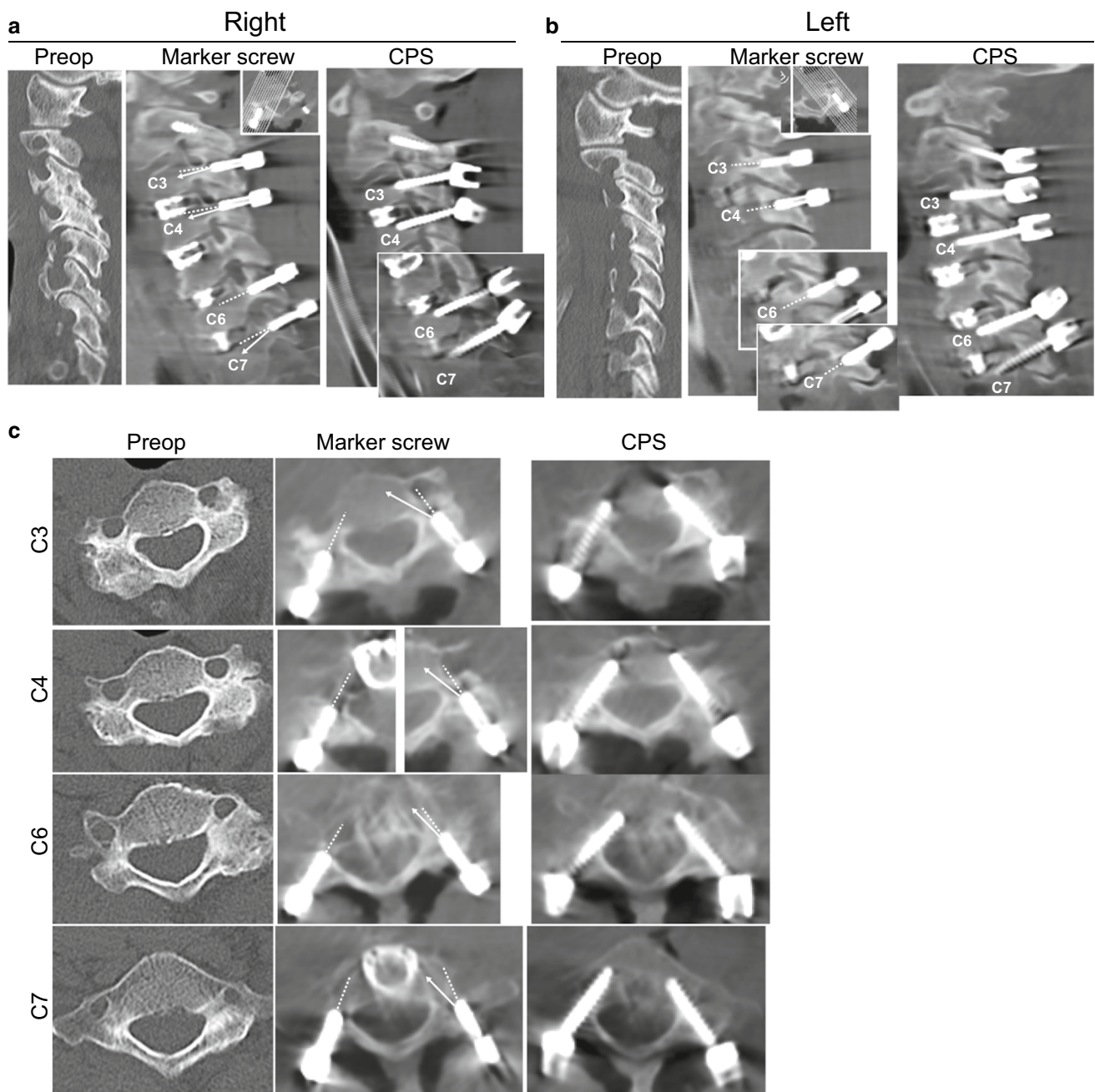


Fig. 6 A 65-year-old woman with athetotic cerebral palsy developed cervical myelopathy caused by degenerative spondylolisthesis. She underwent combined anterior and posterior decompression and fusion using CPSs. Sagittal reconstruction CT-like images along right-side pedicles (a) left-side pedicles (b), and axial CT-like images at C3, C4, C6, and C7 are shown. Preoperative CT-like images show rotational deformity, facet joint degeneration as well as hyperostosis of lateral mass, which made CPS placement difficult. On the CT-like

images with the marker screws, white dotted lines indicate the trajectory of marker screws and white arrows indicate the course, which the surgeon corrected to insert the pedicle probe. In this case, the marker screws on the right, headed in the right direction, while the marker screws on the left headed laterally away from the pedicle. Therefore, we inserted curved pedicle probe with its tip pointed inward and placed CPSs in the appropriate position. Left C4 CPSs were judged as G-1 malposition but remained unchanged

obtained from intraoperative CT-like images does not represent virtual reality but actual information, we can completely rely on its guidance. One specific feature of our technique is the use of a custom-made Ti marker screw, by which we

could make the starting point of the pedicle probing close to the target (isthmus of pedicle) (Fig. 1) and visualize the positional relationship between the starting point (bottom of the pilot hole) and the target using intraoperative C-arm

Table 1 Number of CPSs at each spinal level in each pathological condition

Spinal level	RA ^a	Spondylosis	Tumor	Cong. ^b	OPLL ^c	Trauma ^d	Total
C2	34	14	5	4	0	2	59 (0)
C3	3	8	2	2	0	0	15 (0)
C4	6	10 (3)	6	0	2	0	24 (3)
C5	4	12	9	0	4	2	31 (0)
C6	2	13 (1)	5	0	3	2	25 (1)
C7	2	5	3	0	2	0	12 (0)
Total	51 (0)	62 (4)	30 (0)	6 (0)	11 (0)	6 (0)	166 (4)

Values in brackets indicate the number of malpositioned CPSs

^arheumatoid arthritis; ^bcongenital disorders; ^cossification of posterior longitudinal ligament; ^dspinal trauma

CBCT multiplanar images. The 10-mm length of the Ti marker screw is also the key to this procedure. Based on our CT-based anatomical study and earlier studies [22, 23], the critical range on pedicle screw path is 10–18 mm deep from the entry point on lateral mass at C3–6 level (Supplemental Table 1). Therefore, the Ti marker screw with a length of 10 mm enabled us to create a pilot hole avoiding vertebral artery injury. Since the bottom of pilot hole and the entry of pedicle are very close, it was convenient for us to place the pedicle probe in the pilot hole and penetrate the pedicle by adjusting the direction of pedicle probe according to intraoperative CT-like images. Importantly, we should pay particular attention when inserting the pedicle probe for the first 6 mm from the entry point of the pedicle.

Custom-made ball tip guide wire and 3.5 mm cannulated tapping drill are also helpful for safer and more accurate CPS placement. Vertebral artery injury is more likely to occur during tapping the screw path especially when pulling back the tapping drill because medial wall of the pedicle is always thick and hard while lateral wall of the pedicle is thinner and easy to violate [24]. To avoid violation of pedicle during tapping the procedure, we believe that it is beneficial to use the guidewire.

The results of this study demonstrated that the C-arm CBCT-guided CPS placement can ensure its safety as well as provide a more reliable anchor for cervical spinal reconstruction compared to conventional freehand CPS placement under lateral fluoroscopy despite some potential bias in historical controls who underwent surgery at different periods of time. Although the technique could not achieve 100% accuracy in CPS placement, the absence of any critical G-2 malposition encourages us to use this technique for cervical reconstruction surgery. Other recent techniques of CPS placement such as CT-based navigation system or 3D printing navigation template have successfully improved the accuracy of CPS placement [13–16, 18, 25, 26]. However, we should exert care when using navigation systems because virtual reality is not always accurate in cases with poor fixation of reference frame to cervical vertebra. 3D printing navigation template is also useful in finding the entry point

as well as in creating a screw path, but soft tissues including cartilaginous and ligamentous tissue may interfere with fitting the template to bone leading to errors in CPS trajectory. Given that a small error can lead to critical complications such as vertebral artery injury, it is reasonable to confirm the trajectory of CPS by intraoperative C-arm CBCT before penetrating the pedicle. Additionally, our data showing that 43% of CPS required re-adjustment of the screw trajectory after examining the marker screw trajectory by 1st CBCT scan, emphasize the usefulness of intraoperative C-arm CBCT-guided placement.

Our data also suggest that C-arm CBCT-guided CPS placement is particularly useful when treating patients with RA, in which poor bone quality jeopardizes other anchor solutions. An earlier study showed that among various pathological conditions, RA was associated with the highest screw misplacement rate (26.7%) by the freehand technique [2], while there was no screw malposition in RA patients of this study when using the C-arm CBCT-guided placement technique. As reported previously, the high misplacement rate by freehand technique in RA may be derived from the difficulty in finding the entry points of CPSs due to destructive changes in the lateral mass of cervical spine and from unawareness of breaching the pedicle wall due to severe bone fragility. Therefore, a combination of CT-based preoperative planning of the entry point and intraoperative C-arm CBCT-guided placement technique seems reasonable for accurate placement of CPS in RA patients. However, it should be noted that even though CPS is inserted under the C-arm CBCT-guided placement technique, misplacement of CPS may occur in patients with degenerative spinal disorders along with sclerotic changes on the ideal screw path. In such cases, it is difficult to sense the trabecular channel of the pedicle by probing. Even in such cases, intraoperative C-arm CBCT can inform us the direction we should dig the sclerotic pedicle to create the screw path.

C-arm CBCT-guided CPS placement has an advantage over freehand placement from the perspective of the learning curve. Intraoperative CT-like image guidance helps to compensate for less experience with CPS placement. Yoshimoto

et al. [27] reported that freehand CPS placement using lateral fluoroscopy requires a learning curve of more than 36 cases of experience. Therefore, it is recommended for surgeons with less experience to use any supportive tools available when inserting a CPS to avoid lethal complications during the learning period. The combination of intraoperative CT-like images and marker screws provides immediate feedback regarding the trajectory to the surgeon and helps improve the insertion technique.

One disadvantage of using the C-arm CBCT-guided placement technique is increased radiation exposure compared with conventional freehand CPS placement under lateral fluoroscopy. However, considering the severity of complications associated with CPS malposition, the use of intraoperative C-arm CBCT is justified if safety can be guaranteed. This study demonstrated that C-arm CBCT-guided placement not only decreased the risk for neurovascular injury but also reduced surgery-related complications leading to a lower probability of reoperation. Since reoperation raises both physiological and mental burden on patients as well as increases medical costs and prolongs hospital stays, it can be safely believed that benefits of using C-arm CBCT-guided placement of CPS outweigh its disadvantages.

Of note is that CBCT, which is performed with a C-arm and flat-panel detector, can calculate and reconstruct CT-like images using a lower radiation dose compared with conventional multidetector helical CT. In addition, the average radiation dose of 103 mGy and estimated effective dose of 9.7 ± 6.5 mSv during surgery, including CBCT and lateral fluoroscopy twice, are considered acceptable for adult patients compared with the radiation doses of other spinal procedures. Kobayashi et al. reported an intraoperative radiation dose in spinal scoliosis surgery using the O-arm[®] of 401 mGy on average, and the radiation dose from the preoperative CT scan was 460 mGy on average [28]. Su et al. [29] reported that the total effective dose per O-arm[®]-assisted posterior spine surgery using the default protocol was 12.79 mSv on average. Gebhard et al. [30] reported median radiation doses of 432 mGy in CT-based (3-D) navigation surgery, 664 mGy in C-arm-based (2-D fluoroscopy) computer-assisted navigation surgery, and 152 mGy in Iso-C3D C-arm-based navigation surgery. Safee et al. [31] reported average radiation doses in minimally invasive transforaminal lumbar interbody fusion surgery using intraoperative CT-based navigation of 62.0 mGy. In younger patients, however, we should consider using radiation dose reduction protocols for intraoperative C-arm CBCT. Based on data from recent studies, radiation doses of intraoperative C-arm CBCT can be reduced compared to the manufacturer settings without a negative impact on image quality with regard to information required for spine surgery in pediatric patients [29, 32, 33].

In conclusion, we introduced a new intraoperative C-arm CBCT-guided CPS placement technique, by which the

trajectory of pilot hole can be visualized using a custom-made Ti marker screw, and the trajectory of CPS can be adjusted before penetrating the critical range on CPS path. This novel technique enables intraoperative adjustment of the trajectory of the CPS as well as confirmation of the CPS path before penetrating the isthmus of the pedicle, resulting in accurate and safe CPS placement.

Compliance with ethical standards


Conflict of interest All authors state that they have no conflict of interest.

References

- Hasegawa K, Hirano T, Shimoda H, Homma T, Morita O (2008) Indications for cervical pedicle screw instrumentation in non-traumatic lesions. *Spine* 33:2284–2289. <https://doi.org/10.1097/BRS.0b013e31818043ce>
- Hojo Y, Ito M, Suda K, Oda I, Yoshimoto H, Abumi K (2014) A multicenter study on accuracy and complications of freehand placement of cervical pedicle screws under lateral fluoroscopy in different pathological conditions: CT-based evaluation of more than 1,000 screws. *Eur Spine J* 23:2166–2174. <https://doi.org/10.1007/s00586-014-3470-0>
- Neo M, Sakamoto T, Fujibayashi S (2005) The clinical risk of vertebral artery injury from cervical pedicle screw inserted in degenerative vertebrae. *Spine* 30:2800–2805
- Yukawa Y, Kato F, Ito K, Horie Y, Hida T, Nakashima H, MacHino M (2009) Placement and complications of cervical pedicle screws in 144 cervical trauma patients using pedicle axis view techniques by fluoroscope. *Eur Spine J* 18:1293–1299. <https://doi.org/10.1007/s00586-009-1032-7>
- Dunlap BJ, Karaikovic EE, Park HS, Sokolowski MJ, Zhang LQ (2010) Load sharing properties of cervical pedicle screw-rod constructs versus lateral mass screw-rod constructs. *Eur Spine J* 19:803–808. <https://doi.org/10.1007/s00586-010-1278-0>
- Ito Z, Higashino K, Kato S, Kim SS, Wong E, Yoshioka K, Hutton WC (2014) Pedicle screws can be 4 times stronger than lateral mass screws for insertion in the midcervical spine: a biomechanical study on strength of fixation. *J Spinal Disord Tech* 27:80–85. <https://doi.org/10.1097/BSD.0b013e31824e65f4>
- Jeanneret B, Gebhard JS, Magerl F (1994) Transpedicular screw fixation of articular mass fracture-separation: results of an anatomical study and operative technique. *J Spinal Disord* 7(3):222–229
- Rhee JM, Kraiwattanapong C, Hutton WC (2005) A comparison of pedicle and lateral mass screw construct stiffnesses at the cervicothoracic junction: a biomechanical study. *Spine* 30(21):40
- Abumi K, Kaneda K (1997) Pedicle screw fixation for nontraumatic lesions of the cervical spine. *Spine* 22:1853–1863
- Abumi K, Ito M, Sudo H (2012) Reconstruction of the subaxial cervical spine using pedicle screw instrumentation. *Spine* 37:349–356. <https://doi.org/10.1097/BRS.0b013e318239cf1f>
- Xu R, Ebraheim NA, Skie M (2008) Pedicle screw fixation in the cervical spine. *Am J Orthop* 37:403–408
- Xu RM, Ma WH, Wang Q, Zhao LJ, Hu Y, Sun SH (2009) A free-hand technique for pedicle screw placement in the lower cervical spine. *Orthop Surg* 1:107–112. <https://doi.org/10.1111/j.1757-7861.2009.00023.x>

13. Ishikawa Y, Kanemura T, Yoshida G, Matsumoto A, Ito Z, Tauchi R, Muramoto A, Ohno S, Nishimura Y (2011) Intraoperative, full-rotation, three-dimensional image (O-arm)-based navigation system for cervical pedicle screw insertion. *J Neurosurg, Spine* 15(5):472–478. <https://doi.org/10.3171/2011.6.SPINE10809>
14. Kotani Y, Abumi K, Ito M, Minami A (2003) Improved accuracy of computer-assisted cervical pedicle screw insertion. *J Neurosurg* 99:257–263. <https://doi.org/10.3171/spi.2003.99.3.0257>
15. Tian W, Liu Y, Zheng S, Lv Y (2013) Accuracy of lower cervical pedicle screw placement with assistance of distinct navigation systems: a human cadaveric study. *Eur Spine J* 22:148–155. <https://doi.org/10.1007/s00586-012-2494-6>
16. Fomekong E, Safi S, Raftopoulos C (2017) Spine navigation based on 3-dimensional robotic fluoroscopy for accurate percutaneous pedicle screw placement: a prospective study of 66 consecutive cases. *World Neurosurg* 108:76–83. <https://doi.org/10.1016/j.wneu.2017.08.149>
17. Gebhard F, Riepl C, Richter P, Liebold A, Gorki H, Wirtz R, König R, Wilde F, Schramm A, Kraus M (2012) Der Hybrid-operationssaal. *Der Unfallchirurg* 115(2):107–120. <https://doi.org/10.1007/s00113-011-2118-3>
18. Hecht AC, Koehler SM, Laudone JC, Jenkins A, Qureshi S (2011) Is intraoperative CT of posterior cervical spine instrumentation cost-effective and does it reduce complications? *Clin Orthop Relat Res* 469(4):1035–1041. <https://doi.org/10.1007/s1199-9-010-1603-2>
19. Richter PH, Yarboro S, Kraus M, Gebhard F (2015) One year orthopaedic trauma experience using an advanced interdisciplinary hybrid operating room. *Injury* 46(Suppl 4):34. [https://doi.org/10.1016/S0020-1383\(15\)30032-2](https://doi.org/10.1016/S0020-1383(15)30032-2)
20. International Commission on Radiological Protection (ICRP) (2007) The 2007 Recommendations of the International Commission on Radiological Protection. ICRP publication 103. *Annals of the ICRP* 37(2–4):331–332. <https://doi.org/10.1016/j.icrp.2007.10.003>
21. Deak PD, Smal Y, Kalender WA (2010) Multisection CT protocols: sex- and age-specific conversion factors used to determine effective dose from dose-length product. *Radiology* 257(1):158–166. <https://doi.org/10.1148/radiol.10100047>
22. Tan SH, Teo EC, Chua HC (2004) Quantitative three-dimensional anatomy of cervical, thoracic and lumbar vertebrae of Chinese singaporeans. *Eur Spine J* 13:137–146. <https://doi.org/10.1007/s00586-003-0586-z>
23. Wasinpongwanich K, Paholpak P, Tuamsuk P, Sirichativapee W, Wisanuyotin T, Kosuwon W, Jeeravipoolvarn P (2014) Morphological study of subaxial cervical pedicles by using three-dimensional computed tomography reconstruction image. *Neurol Med-Chir* 54:736–745. <https://doi.org/10.2176/nmc.0a.2013-0287>
24. Karaikovic EE, Yingsakmongkol W, Gaines RW (2001) Accuracy of cervical pedicle screw placement using the funnel technique. *Spine* 26:2456–2462. <https://doi.org/10.1097/00007632-200111150-00012>
25. Guo F, Dai J, Zhang J, Ma Y, Zhu G, Shen J, Niu G (2017) Individualized 3D printing navigation template for pedicle screw fixation in upper cervical spine. *PLoS ONE* 12:1–12. <https://doi.org/10.1371/journal.pone.0171509>
26. Kaneyama S, Sugawara T, Sumi M (2015) Safe and accurate midcervical pedicle screw insertion procedure with the patient-specific screw guide template system. *Spine* 40:E341–E348. <https://doi.org/10.1097/BRS.0000000000000772>
27. Yoshimoto H, Sato S, Hyakumachi T, Yanagibashi Y, Kanno T, Masuda T (2009) Clinical accuracy of cervical pedicle screw insertion using lateral fluoroscopy: a radiographic analysis of the learning curve. *Eur Spine J* 18:1326–1334. <https://doi.org/10.1007/s00586-009-1109-3>
28. Kobayashi K, Ando K, Ito K, Tsushima M, Morozumi M, Tanaka S, Machino M, Ota K, Ishiguro N, Imagama S (2018) Intraoperative radiation exposure in spinal scoliosis surgery for pediatric patients using the O-arm® imaging system. *Eur J Orthop Surg Traumatol*. <https://doi.org/10.1007/s00590-018-2130-1>
29. Su AW, Luo TD, McIntosh AL, Schueler BA, Winkler JA, Stans AA, Larson AN (2016) Switching to a pediatric dose O-arm protocol in spine surgery significantly reduced patient radiation exposure. *J Pediatr Orthop* 36(6):621–626. <https://doi.org/10.1097/BPO.0000000000000504>
30. Gebhard FT, Kraus MD, Schneider E, Liener UC, Kinzl L, Arand M (2006) Does computer-assisted spine surgery reduce intraoperative radiation doses? *Spine* 31(17):2024–2027. <https://doi.org/10.1097/01.brs.0000229250.69369.ac>
31. Safaee MM, Oh T, Pekmezci M, Clark AJ (2018) Radiation exposure with hybrid image-guidance-based minimally invasive transforaminal lumbar interbody fusion. *J Clin Neurosci* 48:122–127. <https://doi.org/10.1016/j.jocn.2017.09.026>
32. Abul-Kasim K, Söderberg M, Selariu E, Gunnarsson M, Kherad M, Ohlin A (2012) Optimization of radiation exposure and image quality of the cone-beam O-arm intraoperative imaging system in spinal surgery. *J Spinal Disord Tech* 25(1):52–58. <https://doi.org/10.1097/BSD.0b013e318211fdea>
33. Petersen A, Eiskjær S, Kaspersen J (2012) Dose optimisation for intraoperative cone-beam flat-detector CT in paediatric spinal surgery. *Pediatr Radiol* 42(8):965–973. <https://doi.org/10.1007/s00247-012-2396-0>

Affiliations

Masahiko Takahata¹  · Katsuhisa Yamada¹ · Iwata Akira¹ · Tsutomu Endo¹ · Hideki Sudo¹ · Hidetoki Yokoyama² · Norimasa Iwasaki¹

✉ Masahiko Takahata
takamasa@med.hokudai.ac.jp

² Department of Radiological Technology, Hokkaido University Hospital, Sapporo, Japan

¹ Department of Orthopedic Surgery, Hokkaido University Graduate School of Medicine, Kita-15 Nishi-7, Kita-ku, Sapporo 060-8638, Japan